

Magnetostructural Correlations in Bis(μ_2 -phenoxide)-Bridged Macrocyclic Dinuclear Copper(II) Complexes. Influence of Electron-Withdrawing Substituents on Exchange Coupling

Laurence K. Thompson,* Sanat K. Mandal, Santokh S. Tandon, John N. Bridson, and Murray K. Park

Department of Chemistry, Memorial University of Newfoundland, St. John's, Newfoundland, A1B 3X7 Canada

Received November 2, 1995[⊗]

Macrocyclic dicopper(II) complexes derived from 2,6-di(R)formylphenols and various linking diamines are surveyed and their magnetic and structural properties assessed. For those systems with "flat" dinuclear centers and no electronic perturbations associated with electron-withdrawing ligands or ligand groups, the complexes exhibit a "straight-line" relationship between exchange integral and phenoxide bridge angle. Within the angle range 98.8–104.7°, 11 complexes are included with $-2J$ in the range 689–902 cm^{-1} . When electron-withdrawing species are present, either as ligands or as groups bound to the macrocycle itself, considerable suppression of the antiferromagnetic exchange component is observed. Single-crystal X-ray diffraction studies are reported for three complexes. $[\text{Cu}_2(\text{L1})(\text{H}_2\text{O})_2]\text{F}_2(\text{CH}_3\text{OH})_2$ (**1**) crystallized in the triclinic system, space group $P\bar{1}$, with $a = 8.1878(5)$ Å, $b = 9.0346(7)$ Å, $c = 10.4048(7)$ Å, $\alpha = 103.672(6)^\circ$, $\beta = 101.163(5)^\circ$, $\gamma = 104.017(5)^\circ$, and $Z = 1$. $[\text{Cu}_2(\text{L2})\text{Cl}_2][\text{Cu}_2(\text{L2})(\text{H}_2\text{O})_2]\text{Cl}(\text{ClO}_4) \cdot 5.5\text{H}_2\text{O}$ (**2**) crystallized in the monoclinic system, space group $P2_1/n$, with $a = 14.4305(5)$ Å, $b = 24.3149(8)$ Å, $c = 18.6584(8)$ Å, $\beta = 111.282(3)^\circ$, and $Z = 4$. $[\text{Cu}_2(\text{L3})(\text{H}_2\text{O})_2](\text{BF}_4)_2$ (**3**) crystallized in the triclinic system, space group $P\bar{1}$, with $a = 8.6127(4)$ Å, $b = 8.6321(7)$ Å, $c = 10.8430(10)$ Å, $\alpha = 74.390(10)^\circ$, $\beta = 86.050(10)^\circ$, $\gamma = 76.350(10)^\circ$, and $Z = 2$. Square pyramidal copper ion stereochemistries are observed in all cases, with axially coordinated halogens or water molecules. Strong antiferromagnetic exchange is observed for all complexes ($-2J = 784(8)$ cm^{-1} , Cu–O–Cu 103.65(10)° (**1**); $-2J = 801(11)$ cm^{-1} , Cu–O–Cu 102.4(3), 107.5(3), 102.9(3), 106.1(3)° (**2**); $-2J = 689(3)$ cm^{-1} , Cu–O–Cu 98.8(4)° (**3**)). The presence of electron-withdrawing CN groups on the periphery of the macrocyclic ligand leads to substantially reduced antiferromagnetic exchange.

Introduction

Magnetostructural correlations in dinuclear copper(II) complexes bridged equatorially by pairs of hydroxide¹ or alkoxide^{2,3} groups show that the major factor controlling spin coupling between the $S = 1/2$ metal centers is the Cu–O(R)–Cu angle. A good linear relationship for the dihydroxide case¹ and an apparent linear relationship for the alkoxide cases^{2,3} show that at angles around 97° the exchange integral approaches zero, the point of experimental "accidental orthogonality". These experimental observations are consistent with extended Hückel MO treatments by Hoffmann⁴ and Kahn.⁵ More recent *ab initio* calculations on simple model dimers examined the effects of bridge angle, Cu–O distance, fold angle along the O–O axis, solid angle at the oxygen bridge, and degree of tetrahedral distortion at the copper centers.^{3,6} The theoretical studies showed that the major factor affecting exchange was the Cu–O–Cu bridge angle, but significant tetrahedral copper distortion and pyramidal distortion, e.g. at the alkoxide bridge, can lead to increased ferromagnetic contributions, which effectively reduce any antiferromagnetic term associated with the alkoxide bridges. Electronic perturbations involving bound ligands with

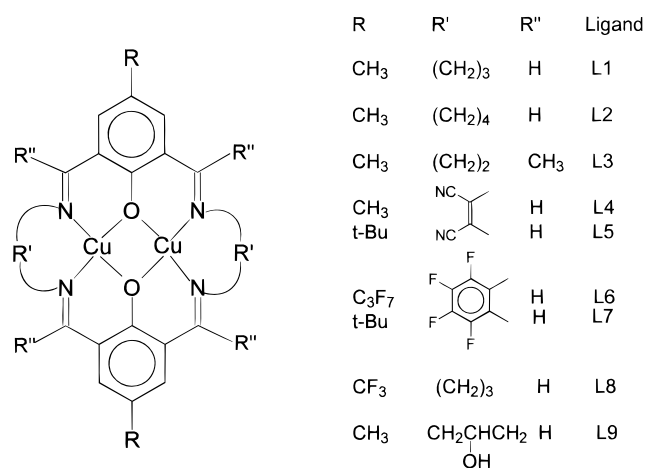


Figure 1. Macrocyclic complexes.

varying electronegativity were also predicted to influence exchange, with antiferromagnetic coupling decreasing as $\text{Br} > \text{Cl} > \text{F}$.⁶ While magnetostructural correlations are well established for simple "open" dimeric species involving two magnetic oxygen bridges, e.g. hydroxide,¹ a similar correlation has not been established for a comparable macrocyclic dicopper(II) system. "Robson" type macrocyclic complexes,⁷ formed by copper ion template condensation of diformylphenols and various diamines (Figure 1), contain phenoxide oxygen atoms bridging the two copper centers and represent ideal systems to

* Author to whom correspondence should be addressed.

[⊗] Abstract published in *Advance ACS Abstracts*, May 1, 1996.

- (1) Crawford, V. H.; Richardson, H. W.; Wasson, J. R.; Hodgson, D. J.; Hatfield, W. E. *Inorg. Chem.* **1976**, *15*, 2107.
- (2) Merz, L.; Haase, W. *J. Chem. Soc., Dalton Trans.* **1980**, 875.
- (3) Handa, M.; Koga, N.; Kida, S. *Bull. Chem. Soc. Jpn.* **1988**, *61*, 3853.
- (4) Hay, P. J.; Thibeault, J. C.; Hoffmann, R. *J. Am. Chem. Soc.* **1975**, *97*, 4884.
- (5) Kahn, O. *Inorg. Chim. Acta* **1982**, *62*, 3.
- (6) Astheimer, H.; Haase, W. *J. Chem. Phys.* **1986**, *85*, 1427.

(7) Pilkington, N. H.; Robson, R. *Aust. J. Chem.* **1970**, *23*, 2225.

examine the exchange coupling via phenoxide oxygen. The degree of distortional flexibility available to simple dimeric copper complexes with hydroxide or alkoxide bridges would be expected to be reduced when the Cu–(O)₂–Cu entity is enclosed within the cavity of a macrocyclic ligand, and so one might expect a more straightforward relationship between e.g. bridge angle and exchange and also with respect to electronic perturbations.

In this report, the existing macrocyclic dicopper(II) complexes of this type are examined structurally and magnetically, in addition to several new complexes, and compared with the simple dimeric dihydroxy-bridged systems and also a series of comparable macrocyclic, phenoxide-bridged dinickel complexes reported recently, for which a straight-line relationship was established between *J* and Ni–O–Ni angle, with a crossover from antiferromagnetic to ferromagnetic behavior occurring at 97°.⁸ Electronic effects associated with directly bonded and remote electron-withdrawing groups will also be assessed.

Experimental Section

Physical Measurements. Electronic spectra were recorded as Nujol mulls and in solution using a Cary 5E spectrometer. Infrared spectra were recorded as Nujol mulls using a Mattson Polaris FT-IR instrument. Microanalyses were carried out by Canadian Microanalytical Service, Delta, Canada. Room-temperature magnetic susceptibilities were measured by the Faraday method using a Cahn 7600 Faraday magnetic balance, and variable-temperature magnetic data (4–305 K) were obtained using an Oxford Instruments superconducting Faraday spectrometer with a Sartorius 4432 microbalance. A main solenoid field of 1.5 T and a gradient field of 10 T m⁻¹ were employed. The magnetic measurements were carried out on the same uniform samples that were analyzed structurally.

Preparations. (a) [Cu₂(L1)(H₂O)₂]F₂(CH₃OH)₂ (**1**). 4-Methyl-2,6-diformylphenol⁹ (0.66 g, 4.0 mmol) dissolved in hot dry methanol (50 mL) was added to a suspension of CuF₂ (0.41 g, 4.0 mmol) in dry methanol (50 mL). A solution of 1,3-diaminopropane (0.45 g, 6.0 mmol) in dry methanol (50 mL) was then added and the mixture refluxed for 7 h, during which the CuF₂ gradually dissolved. The green solution was filtered hot and allowed to stand at room temperature. Green crystals formed (yield 70%). Anal. Calcd for [Cu₂(C₂₄H₂₆N₄O₂)(H₂O)₂]F₂(CH₃OH)₂ (**1**): C, 46.78; H, 5.69; N, 8.38. Found: C, 46.43; H, 5.77; N, 8.51.

(b) [Cu₂(L2)Cl₂][Cu₂(L2)(H₂O)₂]Cl(ClO₄)₂·5.5H₂O (**2**). **2** was synthesized by adding an aqueous solution of NaCl to an aqueous solution of [Cu₂(L2)](ClO₄)₂¹⁰ and obtained as green crystals directly from the reaction mixture.

(c) [Cu₂(L3)(H₂O)₂](BF₄)₂ (**3**). This complex was prepared according to a published procedure,¹¹ and suitable green crystals were obtained for a structural analysis. The structural analysis was repeated to ensure that the structure of the sample used for variable-temperature magnetic measurements was known.

(d) [Cu₂(L4)](ClO₄)₂·3H₂O·CH₃OH (**4**) and [Cu₂(L5)](ClO₄)₂ (**5**). 4-Methyl-2,6-diformylphenol⁹ (0.164 g, 1.00 mmol) and Cu(ClO₄)₂·6H₂O (0.371 g, 1.00 mmol) were dissolved together in methanol (75 mL), and the mixture was refluxed for 5 min, forming a yellow solution. Diaminomaleonitrile (Aldrich) (0.108 g, 1.00 mmol) dissolved in methanol (20 mL) was added dropwise and the mixture refluxed for 48 h. A dark red-brown solution formed, depositing a deep purple-brown solid, which was filtered off, washed with methanol, and dried under vacuum. Yield: 0.33 g, 81%. Anal. Calcd for [Cu₂(C₂₆H₁₄N₈O₂)](ClO₄)₂·3H₂O·CH₃OH (**4**): C, 36.74; H, 2.75; N, 12.70; Cu, 14.41. Found: C, 36.51; H, 2.48; N, 12.94; Cu, 14.66. **5** was prepared in a similar manner using 4-*tert*-butyl-2,6-diformylphenol. Yield: 45%.

Table 1. Summary of Crystallographic Data for [Cu₂(L1)(H₂O)₂]F₂(CH₃OH)₂ (**1**), [Cu₂(L2)Cl₂][Cu₂(L2)(H₂O)₂]Cl(ClO₄)₂·5.5H₂O (**2**), and [Cu₂(L3)(H₂O)₂](BF₄)₂ (**3**)

	1	2	3
empirical formula	C ₂₆ H ₃₈ N ₄ O ₆ ·F ₂ Cu ₂	C ₅₂ H ₇₄ N ₈ O _{15.5} ·Cl ₄ Cu ₄	C ₁₃ H ₁₇ N ₂ O ₂ ·F ₄ BCu
fw	667.69	1455.18	383.64
space group	<i>P</i> 1	<i>P</i> 2 ₁ / <i>n</i>	<i>P</i> 1
<i>a</i> (Å)	8.1878(5)	14.4305(5)	8.6127(4)
<i>b</i> (Å)	9.0346(7)	24.3149(8)	8.6321(7)
<i>c</i> (Å)	10.4048(7)	18.6584(8)	10.8430(10)
α (deg)	103.672(6)		74.390(10)
β (deg)	101.163(5)	111.282(3)	86.050(10)
γ (deg)	104.017(5)		76.350(10)
<i>V</i> (Å ³)	699.44(8)	6100.3(4)	754.4(6)
ρ_{calcd} (g cm ⁻³)	1.585	1.584	1.689
<i>Z</i>	1	4	2
μ (mm ⁻¹)	2.36	0.80	1.50
λ (Å)	1.540 56	0.709 30	0.709 30
<i>T</i> (°C)	25	25	25
<i>R</i> ^a	0.039	0.053	0.087
<i>R</i> _w ^b	0.041	0.057	0.099

$$^a R = \sum ||F_o| - |F_c|| / \sum |F_o|, \quad ^b R_w = [(\sum w(|F_o| - |F_c|)^2) / \sum w F_o^2]^{1/2}.$$

Anal. Calcd for [Cu₂(C₃₂H₂₈N₈O₂)](ClO₄)₂ (**5**): C, 43.64; H, 2.98; N, 12.72; Cu, 14.43. Found: C, 43.24; H, 3.05; N, 12.64; Cu, 14.45.

Safety Note! Perchlorate complexes are potentially explosive, and caution should be exercised when such derivatives are handled. However, the small quantities used in this study were not found to present a hazard. In our laboratory, small quantities of perchlorate complexes are routinely tested for their explosive potential by controlled mechanical impact.

Crystallographic Data Collection and Refinement of the Structures. (a) [Cu₂(L1)(H₂O)₂]F₂(CH₃OH)₂ (**1**). The diffraction intensities of a green crystal of **1** of approximate dimensions 0.20 × 0.20 × 0.20 mm were collected with graphite-monochromatized Cu K α radiation by using the $\theta/2\theta$ scan technique with profile analysis¹² to $2\theta_{\text{max}} = 120.0^\circ$ on an Enraf Nonius CAD4 diffractometer at 295 K. A total of 3199 reflections were measured, of which 2091 were unique and 2055 were considered significant with $I_{\text{net}} > 2.5\sigma(I_{\text{net}})$. Lorentz and polarization factors were applied, but no correction was made for absorption. The cell parameters were obtained by the least-squares refinement of the setting angles of 10 reflections with $2\theta = 110\text{--}120^\circ$ ($\lambda(\text{Cu K}\alpha) = 1.540\ 56\ \text{\AA}$).

The structure was solved by direct methods using MULTAN¹³ and refined by full-matrix least-squares methods to final residuals of $R = 0.039$ and $R_w = 0.041$ for the significant data, with weights based on counting statistics. Hydrogen atoms were placed in calculated positions but not refined. Abbreviated crystal data are given in Table 1, and final positional parameters and equivalent isotropic temperature factors for significant atoms are listed in Table 2. All calculations were performed with the NRCVAX system of programs,¹⁴ and scattering factors were taken from ref 15. A somewhat abnormal thermal motion was observed at carbon atom C(10) (Figure 2), which was pointed out by one reviewer. A disordered model has been considered as an alternative, but when it was refined isotropically, the fit was found to worsen. Also the two partial C(10) atoms that result could not be refined anisotropically without other ellipsoid abnormalities appearing. Therefore the disorder model offers no advantages over the current interpretation. Full listings of experimental and crystal data (Table S1), atomic positional parameters (Table S2), anisotropic thermal parameters (Table S3), and bond distances and angles (Table S4) are included as Supporting Information.

(8) Nanda, K. K.; Thompson, L. K.; Bridson, J. N.; Nag, K. *J. Chem. Soc., Chem. Commun.* **1994**, 1337.

(9) Ullman, F.; Brittner, K. *Chem. Ber.* **1909**, 42, 2539.

(10) Mandal, S. K.; Thompson, L. K.; Newlands, M. J.; Gabe, E. J. *Inorg. Chem.* **1989**, 28, 3707.

(11) Carlisle, W. D.; Fenton, D. E.; Roberts, P. B.; Casellato, U.; Vigato, P. A.; Graziani R. *Transition Met. Chem. (London)* **1986**, 11, 292.

(12) Grant, D. F.; Gabe, E. J. *J. Appl. Crystallogr.* **1978**, 11, 114.

(13) Germain, G.; Main, P.; Woolfson, M. M. *Acta Crystallogr.* **1971**, A27, 368.

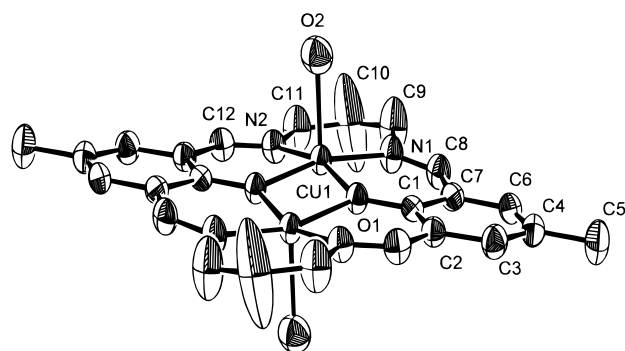
(14) Gabe, E. J.; Lee, F. L.; LePage, Y. In *Crystallographic Computing III*; Sheldrick, G., Kruger, C., Goddard, R., Eds.; Clarendon Press: Oxford, England, 1985; p 167.

(15) *International Tables for X-ray Crystallography*; Kynoch Press: Birmingham, England, 1974; Vol. IV, Table 2.2B, p 99.

Table 2. Final Atomic Positional Parameters and B_{iso} Values for $[\text{Cu}_2(\text{L1})(\text{H}_2\text{O})_2]\text{F}_2(\text{CH}_3\text{OH})_2$ (**1**)

atom	<i>x</i>	<i>y</i>	<i>z</i>	B_{iso}^a (Å ²)
Cu(1)	0.39674(6)	0.32395(5)	0.41361(5)	2.459(22)
O(1)	0.3901(3)	0.50127(24)	0.56486(23)	2.59(10)
O(2)	0.5351(3)	0.2043(3)	0.5391(3)	3.46(12)
N(1)	0.1591(4)	0.1970(3)	0.3990(3)	3.58(14)
N(2)	0.4173(4)	0.1979(3)	0.2372(3)	2.99(13)
C(1)	0.2655(4)	0.5078(4)	0.6291(3)	2.50(16)
C(2)	0.2891(4)	0.6367(4)	0.7446(4)	2.82(16)
C(3)	0.1553(5)	0.6394(4)	0.8110(4)	3.48(18)
C(4)	-0.0031(5)	0.5207(4)	0.7676(4)	3.45(19)
C(5)	-0.1447(6)	0.5275(6)	0.8397(5)	4.92(23)
C(6)	-0.0241(4)	0.3962(4)	0.6545(4)	3.17(17)
C(7)	0.1047(4)	0.3850(4)	0.5849(4)	2.69(15)
C(8)	0.0618(4)	0.2406(4)	0.4730(4)	3.32(16)
C(9)	0.0796(7)	0.0355(6)	0.2974(6)	8.2(3)
C(10)	0.1390(12)	-0.0031(9)	0.1957(8)	16.5(6)
C(11)	0.2839(6)	0.0435(5)	0.1532(4)	5.22(21)
C(12)	0.5542(5)	0.2284(4)	0.1953(4)	3.23(16)

^a B_{iso} is the mean of the principal axes of the thermal ellipsoid.

**Figure 2.** Structural representation for $[\text{Cu}_2(\text{L1})(\text{H}_2\text{O})_2]\text{F}_2(\text{CH}_3\text{OH})_2$ (**1**) with hydrogen atoms omitted (40% probability thermal ellipsoids).

(b) $[\text{Cu}_2(\text{L2})\text{Cl}_2][\text{Cu}_2(\text{L2})(\text{H}_2\text{O})_2]\text{Cl}(\text{ClO}_4) \cdot 5.5\text{H}_2\text{O}$ (**2**). The data collection and structure solution were similar to those for **1**. Hydrogen atoms were placed in calculated positions but not refined. Abbreviated crystal data are given in Table 1, and final positional parameters and equivalent isotropic temperature factors for significant atoms are listed in Table 3. Full listings of experimental and crystal data (Table S1), atomic positional parameters (Table S5), anisotropic thermal parameters (Table S6), and bond distances and angles (Table S7) are included as Supporting Information.

(c) $[\text{Cu}_2(\text{L3})(\text{H}_2\text{O})_2](\text{BF}_4)_2$ (**3**). The data collection and structure solution were to those for similar manner to **1**. Hydrogen atoms were mostly found in difference maps and were allowed to refine in the last three least-squares cycles. The tetrafluoroborate anions were found to be disordered and could not be modeled successfully. The fluorine atoms were found in approximately correct positions and then left unrefined because of the disorder. Abbreviated crystal data are given in Table 1, and final positional parameters and equivalent isotropic temperature factors for significant atoms are listed in Table 4. Full listings of experimental and crystal data (Table S1), atomic positional parameters (Table S8), anisotropic thermal parameters (Table S9), and bond distances and angles (Table S10) are included as Supporting Information.

Results and Discussion

Description of the Structures. (a) $[\text{Cu}_2(\text{L1})(\text{H}_2\text{O})_2]\text{F}_2(\text{CH}_3\text{OH})_2$ (**1**). The structure of **1** is illustrated in Figure 2, and bond distances and angles relevant to the copper coordination spheres are listed in Table 5. The macrocyclic complex adopts an essentially flat structure with the two square pyramidal copper centers bridged by the two phenoxide oxygen atoms, with quite large Cu—O—Cu angles (103.65(10)°). The sum of the angles at the phenoxide oxygens is almost exactly 360° (O(1) 359.8°), indicating no pyramidal oxygen distortion. The copper

Table 3. Final Atomic Positional Parameters and B_{iso} Values for $[\text{Cu}_2(\text{L2})\text{Cl}_2][\text{Cu}_2(\text{L2})(\text{H}_2\text{O})_2]\text{Cl}(\text{ClO}_4) \cdot 5.5\text{H}_2\text{O}$ (**2**)

atom	<i>x</i>	<i>y</i>	<i>z</i>	B_{iso}^a (Å ²)
Cu(1)	0.90297(10)	0.32417(5)	0.00907(7)	2.60(6)
Cu(2)	0.84668(10)	0.20068(5)	-0.02528(7)	2.60(6)
O(1)	0.8392(5)	0.2729(3)	-0.0786(4)	2.7(4)
O(2)	0.9089(5)	0.2525(3)	0.0560(4)	2.7(4)
N(1)	0.8896(6)	0.3853(3)	-0.0611(5)	2.9(4)
N(2)	0.8898(6)	0.3615(3)	0.1021(5)	2.8(4)
N(3)	0.9431(6)	0.1417(3)	0.0303(5)	2.7(4)
N(4)	0.7689(6)	0.1631(4)	-0.1201(5)	3.1(4)
C(1)	0.8090(8)	0.2819(5)	-0.1542(6)	2.8(5)
C(2)	0.7665(8)	0.2402(4)	-0.2073(6)	2.7(5)
C(3)	0.7338(8)	0.2521(5)	-0.2875(6)	3.5(6)
C(4)	0.7447(8)	0.3030(5)	-0.3154(6)	3.8(6)
C(5)	0.7095(8)	0.3124(6)	-0.4008(6)	4.4(7)
C(6)	0.7877(9)	0.3432(5)	-0.2627(6)	3.8(6)
C(7)	0.8199(8)	0.3346(5)	-0.1820(6)	3.2(6)
C(8)	0.8600(8)	0.3811(4)	-0.1341(6)	3.3(6)
C(9)	0.9203(9)	0.4404(5)	-0.0274(7)	4.0(7)
C(10)	0.8326(10)	0.4710(5)	-0.0187(8)	4.8(7)
C(11)	0.7825(9)	0.4370(5)	0.0260(7)	4.3(7)
C(12)	0.8507(9)	0.4179(5)	0.1039(7)	4.2(6)
C(13)	0.9177(8)	0.3364(4)	0.1681(6)	3.0(5)
C(14)	0.9575(7)	0.2810(4)	0.1861(5)	2.1(5)
C(15)	1.0005(8)	0.2670(5)	0.2657(6)	3.1(6)
C(16)	1.0377(8)	0.2154(5)	0.2903(6)	3.1(5)
C(17)	1.0880(9)	0.2030(6)	0.3749(6)	4.4(7)
C(18)	1.0307(8)	0.1766(5)	0.2362(6)	2.9(5)
C(19)	0.9857(7)	0.1873(4)	0.1565(6)	2.5(5)
C(20)	0.9500(7)	0.2409(4)	0.1303(6)	2.3(5)
C(21)	0.9887(8)	0.1443(4)	0.1050(6)	2.8(5)
C(22)	0.9659(9)	0.0940(4)	-0.0097(7)	3.8(7)
C(23)	0.8831(9)	0.0516(5)	-0.0352(7)	4.3(7)
C(24)	0.7991(10)	0.0625(5)	-0.1121(8)	4.6(7)
C(25)	0.7278(9)	0.1074(5)	-0.1181(7)	3.6(6)
C(26)	0.7427(7)	0.1853(4)	-0.1865(6)	2.7(5)
Cl(1)	1.09211(22)	0.33302(14)	0.05354(17)	4.24(16)
Cl(2)	0.7179(3)	0.17593(6)	0.03714(19)	5.20(18)
Cu(3)	0.83734(10)	0.19593(5)	0.45414(7)	2.49(6)
Cu(4)	0.88001(10)	0.32018(5)	0.48761(7)	2.52(6)
O(3)	0.8978(5)	0.2481(3)	0.5403(3)	2.5(4)
O(4)	0.8144(5)	0.2682(3)	0.4064(3)	2.6(4)
N(5)	0.8570(6)	0.1346(3)	0.5248(5)	2.4(4)
N(6)	0.8406(6)	0.1600(4)	0.3576(5)	3.1(5)
N(7)	0.7853(6)	0.3793(4)	0.4329(5)	3.2(4)
N(8)	0.9630(7)	0.3584(3)	0.5805(5)	3.0(4)
C(27)	0.9287(7)	0.2393(4)	0.6163(5)	2.2(5)
C(28)	0.9732(7)	0.2818(4)	0.6691(5)	2.2(5)
C(29)	1.0063(7)	0.2724(4)	0.7485(6)	2.5(5)
C(30)	0.9957(7)	0.2207(5)	0.7770(5)	2.7(5)
C(31)	1.0346(9)	0.2099(5)	0.8635(6)	4.2(6)
C(32)	0.9534(8)	0.1782(5)	0.7241(6)	3.3(6)
C(33)	0.9218(7)	0.1865(4)	0.6450(6)	2.6(5)
C(34)	0.8839(8)	0.1384(4)	0.5985(6)	2.7(5)
C(35)	0.8281(9)	0.0794(4)	0.4933(6)	3.4(6)
C(36)	0.9158(9)	0.0517(5)	0.4800(7)	3.9(7)
C(37)	0.9585(9)	0.0850(5)	0.4296(7)	4.0(7)
C(38)	0.8808(9)	0.1042(5)	0.3554(6)	3.4(6)
C(39)	0.8052(8)	0.1847(5)	0.2922(5)	3.2(6)
C(40)	0.7674(8)	0.2400(5)	0.2757(6)	3.2(6)
C(41)	0.7242(8)	0.2532(5)	0.1980(6)	3.4(6)
C(42)	0.6888(9)	0.3057(6)	0.1733(6)	4.3(7)
C(43)	0.6431(9)	0.3203(6)	0.0892(6)	4.8(7)
C(44)	0.6948(9)	0.3452(5)	0.2297(7)	4.2(6)
C(45)	0.7396(8)	0.3342(5)	0.3085(6)	3.0(5)
C(46)	0.7751(7)	0.2806(5)	0.3315(5)	2.7(5)
C(47)	0.7369(8)	0.3778(4)	0.3603(6)	3.2(6)
C(48)	0.7632(10)	0.4279(5)	0.4732(7)	4.2(7)
C(49)	0.8463(11)	0.4699(5)	0.4949(7)	4.9(8)
C(50)	0.9330(12)	0.4596(6)	0.5703(8)	5.9(9)
C(51)	1.0033(9)	0.4133(5)	0.5742(7)	4.2(6)
C(52)	0.9932(8)	0.3368(5)	0.6474(6)	3.4(6)
O(1H)	0.9964(5)	0.3337(3)	0.4299(4)	3.3(4)
O(2H)	0.6692(5)	0.1785(3)	0.4188(4)	3.4(4)

^a B_{iso} is the mean of the principal axes of the thermal ellipsoid.

Table 4. Final Atomic Positional Parameters and B_{iso} Values for $[\text{Cu}_2(\text{L}3)(\text{H}_2\text{O})_2](\text{BF}_4)_2$ (**3**)

atom	<i>x</i>	<i>y</i>	<i>z</i>	B_{iso}^a (\AA^2)
Cu	0.98253(19)	0.40851(21)	0.63087(15)	3.02(7)
O(1)	1.1348(10)	0.4121(11)	0.4929(8)	3.5(4)
O(2)	1.0931(17)	0.557(3)	0.7456(15)	5.2(8)
N(1)	1.1028(13)	0.2044(13)	0.7311(10)	3.1(5)
N(2)	0.8009(13)	0.3810(13)	0.7354(9)	3.0(5)
C(1)	1.2912(15)	0.3430(15)	0.4998(11)	4.2(6)
C(2)	1.3504(15)	0.2059(15)	0.6063(11)	4.2(6)
C(3)	1.5122(17)	0.1384(19)	0.6082(15)	3.4(7)
C(4)	1.2444(16)	0.1295(16)	0.7092(11)	4.7(7)
C(5)	1.317(3)	−0.0409(22)	0.7904(19)	4.6(9)
C(6)	1.0013(20)	0.1317(21)	0.8325(16)	4.2(8)
C(7)	0.8579(20)	0.2580(23)	0.8554(16)	4.3(8)
C(8)	0.6549(16)	0.4627(16)	0.7173(11)	4.4(7)
C(9)	0.531(3)	0.426(4)	0.8192(23)	5.9(12)
C(10)	1.3974(15)	0.4015(16)	0.4022(12)	4.5(7)
C(11)	1.5606(16)	0.3226(19)	0.4159(15)	3.3(7)
C(12)	1.6190(15)	0.1932(17)	0.5171(13)	3.3(7)
C(13)	1.7942(20)	0.110(3)	0.5262(21)	5.6(10)

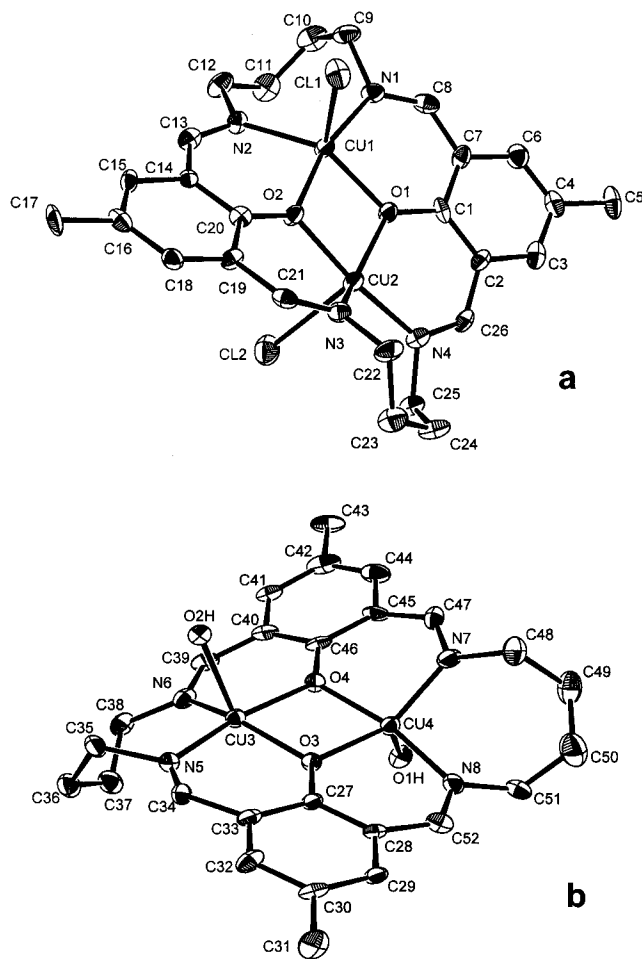
^a B_{iso} is the mean of the principal axes of the thermal ellipsoid.

Table 5. Interatomic Distances (\AA) and Angles (deg) Relevant to the Copper Coordination Spheres in $[\text{Cu}_2(\text{L}1)(\text{H}_2\text{O})_2]\text{F}_2(\text{CH}_3\text{OH})_2$ (**1**)

Cu(1)–O(1)	1.9824(21)	Cu(1)–N(2)	1.980(3)
Cu(1)–O(1) ^a	1.9842(21)	O(1)–Cu(1) ^a	1.9842(21)
Cu(1)–N(1)	1.962(3)	Cu(1)–Cu(1) ^a	3.1184(6)
Cu(1)–O(2)	2.2027(8)		
O(1)–Cu(1)–O(1) ^a	76.35(9)	O(1)–Cu(1)–N(1)	92.27(11)
O(1)–Cu(1)–N(2)	163.09(11)	O(1) ^a –Cu(1)–N(1)	165.02(11)
O(1) ^a –Cu(1)–N(2)	92.04(10)	N(1)–Cu(1)–N(2)	96.77(12)
Cu(1)–O(1)–Cu(1) ^a	103.65(10)		

centers are separated by 3.1184(6) \AA , and in-plane copper–ligand distances fall in the range 1.965–1.99 \AA . Two water molecules occupy axial positions in a trans arrangement with somewhat longer contacts (Cu(1)–O(2) 2.2027(8) \AA), and the copper centers are displaced toward the waters by 0.208 \AA from the mean N_2O_2 basal plane. The fluoride ions and methanol molecules occupy lattice sites, with the water molecules from separate macrocyclic complexes and the methanol molecules hydrogen bonded to the fluoride ions (F(1)–H(2A)(H_2O) 1.74(4) \AA , F(1)–H(3A)(CH_3OH) 1.58(4) \AA ; H(2A)–F(1)–H(3A) 96.9(18) $^\circ$, O(2)–H(2A)–F(1) 167(4) $^\circ$, O(3)–H(3A)–F(1) 176(3) $^\circ$) in an arrangement in which two water molecules and two fluoride ions form an eight-membered ring between each adjacent pair of macrocyclic units. This hydrogen-bonding framework links the macrocyclic complexes in a stepped, trans-axial linear chain (Figure S1; supporting information).

(b) $[\text{Cu}_2(\text{L}2)\text{Cl}_2][\text{Cu}_2(\text{L}2)(\text{H}_2\text{O})_2]\text{Cl}(\text{ClO}_4)\cdot 5.5\text{H}_2\text{O}$ (2**).** The structure of **2** is illustrated in Figure 3, which depicts the two different molecules in the unit cell. Bond distances and angles relevant to the copper coordination spheres are listed in Table 6. The neutral dinuclear macrocyclic complex (Figure 3a) has two highly distorted square pyramidal copper centers bridged by the phenoxide oxygens. Equatorial contacts to the NO donor sets are short (<2.03 \AA), while the axial copper–chlorine distances are much longer (2.557(3), 2.597(4) \AA). The Cu–Cu separation is 3.115(9) \AA , and the Cu–O–Cu angles are 102.4(3) and 107.5(3) $^\circ$. The latter angle (Cu(1)–O(2)–Cu(2)) is very large and substantially larger than any previously recorded for macrocyclic complexes of this sort. This may be attributed to the highly distorted nature of the macrocyclic ligand itself and also the copper coordination spheres. The effect of the C_4 chain linking the azomethine nitrogen donors and the resulting seven-membered chelate ring is to twist the two phenolic residues and the copper basal planes with an angle

**Figure 3.** Structural representation for $[\text{Cu}_2(\text{L}2)\text{Cl}_2]$ (a) and $[\text{Cu}_2(\text{L}2)(\text{H}_2\text{O})_2]^{2+}$ (b) in $[\text{Cu}_2(\text{L}2)\text{Cl}_2][\text{Cu}_2(\text{L}2)(\text{H}_2\text{O})_2]\text{Cl}(\text{ClO}_4)\cdot 5.5\text{H}_2\text{O}$ (**2**), with hydrogen atoms omitted (40% probability thermal ellipsoids).

between the benzene mean planes of 30.7 $^\circ$. Deviations of the NO basal donor sets from the N_2O_2 mean planes lie in the ranges −0.324 to +0.236 \AA (Cu(1)), with a copper displacement of 0.236 \AA from the mean plane, and −0.369 to +0.339 \AA (Cu(2)), with a copper displacement of 0.290 \AA from the mean plane. An angle of 26.6 $^\circ$ exists between the N_2O_2 mean planes. One basal angle at each copper center is very small (O(1)–Cu(1)–N(2) 145.3(3) $^\circ$, O(1)–Cu(2)–N(3) 141.9(3) $^\circ$), indicating significant distortion of the square pyramid toward a trigonal bipyramid. The Addison distortion index (τ)¹⁶ is <0.5 for each copper center (τ : 0.34, Cu(1); 0.41, Cu(2)), and so on balance the coordination geometry at each copper is best described as distorted square pyramidal.

A similar situation prevails for the cation $[\text{Cu}_2(\text{L}2)(\text{H}_2\text{O})_2]^{2+}$ (Figure 3b). The two distorted square pyramidal copper centers are separated by 3.102(1) \AA and bridged by the two phenoxide oxygen atoms with Cu–O–Cu bridge angles of 102.9(3) and 106.1(3) $^\circ$, one of which is quite large. Axial contacts to the two water molecules are somewhat shorter than the axial chlorine contacts found in the other molecule (Cu(3)–O(2H) 2.312(2) \AA , Cu(4)–O(1H) 2.325(2) \AA). A similar twisting of the ligand itself, forced to occur because of the large size of the butane bridging fragment between the azomethine nitrogens, results in an angle of 30.0 $^\circ$ between the benzene ring mean planes. The copper basal coordination planes are again severely distorted, with displacements of the donor atoms around Cu(3)

(16) Addison, A. W.; Rao, T. N.; Reedijk, J.; van Rijn, J.; Verschoor, G. C. *J. Chem. Soc., Dalton Trans.* **1984**, 1349.

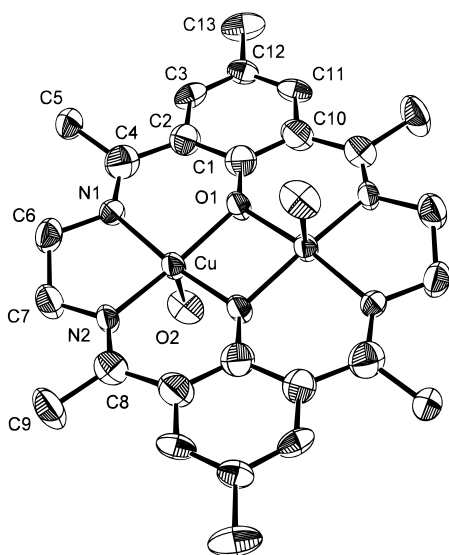


Figure 4. Structural representation for $[\text{Cu}_2(\text{L}3)(\text{H}_2\text{O})_2](\text{BF}_4)_2$ (**3**) with hydrogen atoms omitted (40% probability thermal ellipsoids).

Table 6. Interatomic Distances (Å) and Angles (deg) Relevant to the Copper Coordination Spheres in $[\text{Cu}_2(\text{L}2)\text{Cl}_2][\text{Cu}_2(\text{L}2)(\text{H}_2\text{O})_2]\text{Cl}(\text{ClO}_4)\cdot 5.5\text{H}_2\text{O}$ (**2**)

Cu(1)—O(1)	1.997(7)	Cu(3)—O(3)	1.984(6)
Cu(1)—O(2)	1.938(7)	Cu(3)—O(4)	1.944(6)
Cu(1)—N(1)	1.944(8)	Cu(3)—N(5)	1.943(8)
Cu(1)—N(2)	2.028(8)	Cu(3)—N(6)	2.018(8)
Cu(1)—Cl(1)	2.557(3)	Cu(3)—O(2H)	2.312(2)
Cu(2)—O(1)	2.001(6)	Cu(4)—O(3)	1.980(6)
Cu(2)—O(2)	1.925(6)	Cu(4)—O(4)	1.936(6)
Cu(2)—N(3)	2.006(8)	Cu(4)—N(7)	1.990(9)
Cu(2)—N(4)	1.945(8)	Cu(4)—N(8)	1.949(8)
Cu(2)—Cl(2)	2.597(4)	Cu(4)—O(1H)	2.325(2)
Cu(1)—Cu(2)	3.115(9)	Cu(3)—Cu(4)	3.102(1)
O(1)—Cu(1)—O(2)	74.9(3)	N(3)—Cu(2)—Cl(2)	94.4(3)
O(1)—Cu(1)—N(1)	91.3(3)	N(4)—Cu(2)—Cl(2)	91.6(3)
O(1)—Cu(1)—N(2)	145.3(3)	Cu(1)—O(1)—Cu(2)	102.4(3)
O(1)—Cu(1)—Cl(1)	116.0(2)	Cu(1)—O(2)—Cu(2)	107.5(3)
O(2)—Cu(1)—N(1)	165.8(3)	O(3)—Cu(3)—O(4)	75.2(3)
O(2)—Cu(1)—N(2)	91.0(3)	O(3)—Cu(3)—N(5)	91.6(3)
O(2)—Cu(1)—Cl(1)	93.6(2)	O(3)—Cu(3)—N(6)	148.6(3)
N(1)—Cu(1)—N(2)	102.6(4)	O(4)—Cu(3)—N(5)	164.6(3)
N(1)—Cu(1)—Cl(1)	89.3(3)	O(4)—Cu(3)—N(6)	92.1(3)
N(2)—Cu(1)—Cl(1)	96.1(3)	N(5)—Cu(3)—N(6)	103.2(4)
O(1)—Cu(2)—O(2)	75.1(3)	O(3)—Cu(4)—O(4)	75.5(3)
O(1)—Cu(2)—N(3)	141.9(3)	O(3)—Cu(4)—N(7)	146.6(3)
O(1)—Cu(2)—N(4)	92.9(3)	O(3)—Cu(4)—N(8)	93.1(3)
O(1)—Cu(2)—Cl(2)	120.5(2)	O(4)—Cu(4)—N(7)	91.1(3)
O(2)—Cu(2)—N(3)	91.3(3)	O(4)—Cu(4)—N(8)	167.4(3)
O(2)—Cu(2)—N(4)	166.9(3)	N(7)—Cu(4)—N(8)	101.4(4)
O(2)—Cu(2)—Cl(2)	90.2(2)	Cu(3)—O(3)—Cu(4)	102.9(3)
N(3)—Cu(2)—N(4)	101.4(3)	Cu(3)—O(4)—Cu(4)	106.1(3)
O(3)—Cu(3)—O(2H)	117.2(2)	O(3)—Cu(4)—O(1H)	111.7(2)
O(4)—Cu(3)—O(2H)	92.9(2)	O(4)—Cu(4)—O(1H)	87.7(3)
N(5)—Cu(3)—O(2H)	85.8(2)	N(7)—Cu(4)—O(1H)	97.8(2)
N(6)—Cu(3)—O(2H)	91.6(2)	N(8)—Cu(4)—O(1H)	91.8(3)

in the range -0.327 to $+0.270$ Å and around Cu(4) in the range -0.304 to $+0.309$ Å from their respective mean planes. The mean planes of the basal donor sets are inclined by 28.8° . The copper atoms themselves are displaced toward the coordinated water molecules by 0.220 Å (Cu(3)) and 0.241 Å (Cu(4)). One basal angle at each copper center is quite small (O(3)—Cu(3)—N(6) $148.6(3)^\circ$, O(3)—Cu(4)—N(7) $146.6(3)^\circ$; $\tau = 0.27$ (Cu(3)), 0.34 (Cu(4))), but as in Figure 3a, the coordination geometry at the copper centers is best described as distorted square pyramidal.

(c) $[\text{Cu}_2(\text{L}3)(\text{H}_2\text{O})_2](\text{BF}_4)_2$ (**3**). The structural features of **3** (Figure 4) are essentially the same as those reported previously,¹¹

Table 7. Interatomic Distances (Å) and Angles (deg) Relevant to the Copper Coordination Spheres in $[\text{Cu}_2(\text{L}3)(\text{H}_2\text{O})_2](\text{BF}_4)_2$ (**3**)

Cu—Cu ^a	2.997(3)	Cu—O(2)	2.388(21)
Cu—O(1)	1.919(8)	O(1)—Cu ^a	1.884(8)
Cu—O(1) ^a	1.884(8)	Cu—N(2)	1.891(10)
Cu—N(1)	1.903(10)		
O(1)—Cu—O(2)	98.3(5)	O(1) ^a —Cu—O(2)	99.2(5)
O(2)—Cu—N(1)	90.7(5)	O(2)—Cu—N(2)	98.4(5)
O(1)—Cu—O(1) ^a	81.2(3)	N(1)—Cu—N(2)	90.4(5)
O(1)—Cu—N(1)	92.3(4)	Cu—O(1)—Cu ^a	98.8(4)
O(1)—Cu—N(2)	163.0(5)	O(1) ^a —Cu—N(2)	93.2(4)
O(1) ^a —Cu—N(1)	168.8(5)		

with two square pyramidal copper centers occupying the macrocyclic cavity with an almost planar basal array of donors. Bond distances and angles relevant to the copper coordination spheres are given in Table 7. Cell parameters differ slightly from those reported previously, possibly due to the fact that no additional lattice water molecules were detected in the present structure, and consequently there are slight differences in bond distances and angles. The Cu—Cu separation is $2.997(3)$ Å, and the Cu—O(1)—Cu(A) bridge angle of $98.8(4)^\circ$ is somewhat larger than that reported previously ($96.5(5)^\circ$). Despite the difficulty of modeling the disordered BF_4 anions, the refinement is slightly better in the present case, and so the current phenoxide bridge angle is used in the magnetostructural analysis.

Spectral Data. Infrared spectra of both **4** and **5** show ν (C=N) stretching bands in the range 1570 – 1605 cm^{-1} and the absence of any carbonyl bands associated with the diformylphenol starting materials or nonmacrocyclic intermediates. Diaminomaleonitrile itself has one strong ν (C≡N) stretching frequency at 2210 cm^{-1} , which is replaced in the complexes with two bands, one much stronger than the other, in the same region (2236 (m), 2198 (vw) cm^{-1} (**4**); 2235 (m), 2173 (vw) cm^{-1} (**5**)). Prominent single perchlorate bands at 1099 cm^{-1} (**4**) and 1095 cm^{-1} (**5**) indicate the presence of ClO_4^- ions. Infrared spectral and analytical data (see Experimental Section) clearly indicate the formation of macrocyclic complexes, and given the similarity with **3**, based on chelate ring sizes, a reasonably flat 2:2 macrocycle (cf. L3) is considered to be reasonable. The intense purple-brown colors of **4** and **5** suggest the presence of strong visible absorptions. Solution spectra in MeOH reveal the following bands (nm) (ϵ , $\text{L mol}^{-1} \text{cm}^{-1}$); 475 sh (1.7×10^4), 430 (2.7×10^4), 370 (2.7×10^4), 320 (3.1×10^4) (**4**), 475 (6.7×10^3), 380 (1.6×10^4), 270 (2.9×10^4). Much weaker, less well defined shoulders are found at lower energy, associated with d—d transitions. Such strong absorptions are clearly associated with charge transfer transitions, which reflect the presence of the four cyano groups and also the highly delocalized π macrocyclic framework. The substantial difference between the spectra of the two compounds suggests that the remote 4-alkyl substituents may well be influencing the electronic properties of the complex. Generally complexes of the type $[\text{Cu}_2(\text{L})(\text{ClO}_4)_2]$ (Figure 1; L = L1(R' = Me, Prⁿ, Ph)) are green and exhibit weak visible absorptions (580 – 600 nm) and intense UV absorptions only (350 – 360 nm, $\epsilon = (1.4$ – $1.6) \times 10^4$ $\text{L mol}^{-1} \text{cm}^{-1}$ (CH_3CN)).¹⁷

Attempts to produce X-ray-quality crystals of **4** and **5** have been frustrated by the limited solubility of these compounds in suitable solvents and the fact that the macrocyclic ligand is highly susceptible to reaction with the solvent itself in some cases. Recrystallization of **4** from acetone produced orange-brown crystals, whose infrared spectrum revealed carbonyl stretching bands at 1712 and 1694 cm^{-1} , associated with acetone fragments, and the absence of any band associated with ClO_4^- .

Table 8. Magnetic Data

compd	g	$-2J$ (cm ⁻¹)	ρ	$N\alpha$ (10 ⁶ emu)	Θ (K)	10 ² R^a
[Cu ₂ (L1)(H ₂ O) ₂]F ₂ (CH ₃ OH) ₂ (1)	2.08(4)	784(8)	0.0025	40	-0.2	1.5
[Cu ₂ (L2)Cl ₂][Cu ₂ (L2)(H ₂ O) ₂] Cl(ClO ₄) ₄ ·5.5H ₂ O (2)	2.15(5)	801(11)	0.0003	56	-1.0	1.3
[Cu ₂ (L3)(H ₂ O) ₂](BF ₄) ₂ (3)	2.126(7)	689(3)	0.006	45	0.0	1.1
[Cu ₂ (L4)](ClO ₄) ₂ ·3H ₂ O·CH ₃ OH (4)	2.00(2)	465(4)	0.012	45	-0.3	0.88
[Cu ₂ (L5)](ClO ₄) ₂ (5)	2.05(3)	445(10)	0.03	74	-0.8	2.7

$$^a R = [\sum(\chi_{\text{obs}} - \chi_{\text{calc}})^2 / \sum\chi_{\text{obs}}^2]^{1/2}.$$

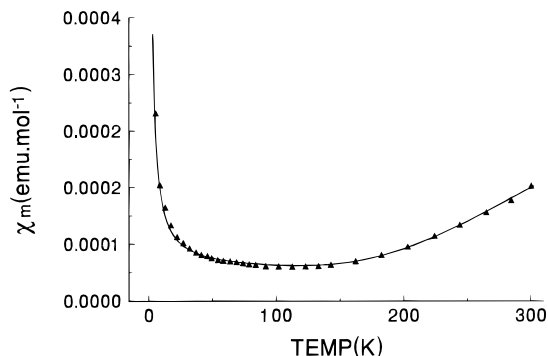


Figure 5. Magnetic data for [Cu₂(L1)(H₂O)₂]F₂(CH₃OH)₂ (**1**). The solid line was calculated from eq 1 with $g = 2.08(4)$, $-2J = 784(8)$ cm⁻¹, $\rho = 0.0025$, $N\alpha = 40 \times 10^{-6}$ emu, $\Theta = -0.2$ K ($10^2R = 1.5$) ($R = [\sum(\chi_{\text{obs}} - \chi_{\text{calc}})^2 / \sum\chi_{\text{obs}}^2]^{1/2}$).

A preliminary X-ray structural analysis on this compound revealed a neutral, dinuclear macrocyclic copper(II) complex, in which two acetone molecules have undergone conjugate addition to two of the imine (C=N) linkages to produce saturated C-N groups, with the ligand bearing four negative charges.¹⁸ The structure however confirms the dinuclear, macrocyclic nature of the parent complex **4**. The acetone adduct is highly distorted, with a saucer-like shape and a significant bending of the dinuclear center along the O-O (phenoxide) axis. The Cu-Cu separation (2.788(2) Å) and the Cu-O-Cu angles (92.0(2), 92.8(3)°) are the smallest known for systems of this sort.

Magnetic Properties. The room-temperature magnetic moments for **1** and **2** are very low ($\mu_{\text{eff}} = 0.51$ and $0.50 \mu_{\text{B}}$, respectively), indicating the likelihood of very strong antiferromagnetic exchange. Variable-temperature magnetic studies on **1** and **2** were carried out in the temperature range 4–300 K, and a plot of molar susceptibility versus temperature for **1** is illustrated in Figure 5. The sharp rise in χ_{m} at low temperature indicates the presence of a small amount of paramagnetic impurity. The variable-temperature susceptibility data were fitted to the Bleaney-Bowers equation (eq 1),¹⁹ using the

$$\chi_{\text{m}} = \frac{N\beta^2 g^2}{3k(T - \Theta)} [1 + 1/3 \exp(-2J/kT)]^{-1} (1 - \rho) + \frac{(N\beta^2 g^2)\rho}{4kT} + N\alpha \quad (1)$$

isotropic (Heisenberg) exchange Hamiltonian ($H = -2JS_1 \cdot S_2$) for two interacting $S = 1/2$ centers (χ_{m} is expressed per mole of copper atoms, $N\alpha$ is the temperature-independent paramagnetism, ρ is the fraction of monomeric impurity, and Θ is a corrective term for interdimer interactions^{20,21}). The best data

fit to eq 1 gave $g = 2.08(4)$, $-2J = 784(8)$ cm⁻¹, $N\alpha = 40 \times 10^{-6}$ emu, $\rho = 0.0025$, and $\Theta = -0.2$ K ($10^2R = 1.5$). The solid line in Figure 5 is calculated from eq 1 using these values (magnetic results for all the complexes studied are listed in Table 8). The very small Θ value indicates that intermolecular exchange effects are essentially nonexistent, in keeping with the axial nature of the hydrogen bonded chain interaction. A similar data fit for **2** gave $g = 2.15(5)$, $-2J = 801(11)$ cm⁻¹, $\rho = 0.0003$, $N\alpha = 56 \times 10^{-6}$ emu, and $\Theta = -1.0$ K ($10^2R = 1.3$). This represents an averaged magnetic analysis, given the fact that there are two distinct molecules in the structure, with four different Cu-O-Ph-Cu angles.

The room-temperature magnetic moment for **3** ($\mu_{\text{eff}} = 0.67 \mu_{\text{B}}$) is somewhat larger than those for **1** and **2** but still indicates the presence of very strong antiferromagnetic exchange. This contrasts somewhat with the previously reported value of $1.44 \mu_{\text{B}}$.¹¹ If this represents the molar value then by conversion $\mu_{\text{eff(Cu)}}$ would be $0.95 \mu_{\text{B}}$, which is substantially higher than our value. Variable-temperature magnetic susceptibility data for **3**, measured in the temperature range 4–300 K, were fitted to eq 1, giving $-2J = 689(3)$ cm⁻¹ (Table 8). It is therefore apparent that, despite the fact that the phenoxide bridge angle for **3** (98.8–(4)°) is close to the crossover point for bis(hydroxy)-bridged dicopper(II) complexes, where at a Cu-OH-Cu angle of 97.5° the magnetic behaviour changes from antiferromagnetic to ferromagnetic,¹ complexes of this sort are clearly still in their antiferromagnetic realm at comparable bridge angles. The earlier structural report for **3** quoted the Cu-O-Cu angle as 96.5(5)°,¹¹ which is even smaller.

Room-temperature magnetic moments for **4** and **5** are substantially higher than those normally observed for macrocyclic complexes of this sort ($\mu_{\text{eff}} = 0.99 \mu_{\text{B}}$ (**4**), $1.05 \mu_{\text{B}}$ (**5**)) but still indicate moderate net antiferromagnetic coupling. Variable-temperature magnetic studies were carried out on **4** and **5** in the temperature range 4–300 K, and the data were fitted to eq 1 in the normal way (Table 8). The $-2J$ values (465(4) cm⁻¹ (**4**); 445(10) cm⁻¹ (**5**)) are substantially smaller than those observed for **1–3**.

Only a few structural examples of complexes of this sort have been reported, in which the linker group between the azomethine nitrogens is two-membered, thus creating a five-membered chelate ring.^{11,22,23} Cu-O_{phenoxide}-Cu angles fall in the range 98.8(4)–100.9(3)°, at the lower end of the range of angles which is typical for such macrocyclic systems. In all cases, the molecules themselves and the dinuclear centers are almost flat. The projected structural similarity between **4** and **5** and these complexes, given the similar nature of the five-membered chelate ring created by the dicyanoethylene fragment, would suggest similar phenoxide bridge angles for **4** and **5**. This being the case, the substantial reduction in $-2J$ values for **4** and **5**, when compared with e.g. **3**, requires an explanation that may not be dependent on structural comparisons per se. The

(18) Park, M. K.; Thompson, L. K. Unpublished results.

(19) Bleaney, B.; Bowers, K. D. *Proc. R. Soc. London* **1952**, A214, 451.

(20) McGregor, K. T.; Barnes, J. A.; Hatfield, W. E. *J. Am. Chem. Soc.* **1973**, 95, 7993.

(21) Sikorav, S.; Bkouche-Waksman, I.; Kahn, O. *Inorg. Chem.* **1984**, 23, 490.

(22) Mandal, S. K.; Thompson, L. K.; Newlands, M. J.; Biswas, A. K.; Adhikary, B.; Nag, K. *Can. J. Chem.* **1989**, 67, 662.

(23) Brychey, K.; Dräger, K.; Jens, K.-J.; Tilset, M.; Behrens, U. *Chem. Ber.* **1994**, 127, 465.

presence of four strongly electron-withdrawing cyano groups positioned in close proximity to the metal magnetic orbitals and immediately adjacent to a highly delocalized π framework suggests that the substantial reduction in exchange results from an electronic perturbation by the cyano groups, which generate significant electropositive character at the copper centers, thus limiting spin coupling.

Numerous studies have focused on macrocyclic complexes derived by template condensation of 2,6-diformylphenols and diamines, since Robson's first report in 1970,⁷ in which 4-methyl-2,6-diformylphenol was cyclized with 1,3-diaminopropane in the presence of Cu, Ni, Co, Mn, Fe, and Zn salts. A somewhat limited series of studies since then has focused on structures and magnetic properties of the dicopper complexes of such macrocyclic ligands (Figure 1; L1–L3, L6–L9),^{11,21–31} but so far, there has been no attempt to develop a magneto-structural correlation. A plot of the existing magnetic and structural data (averaged Cu–O–Cu angles are quoted when the two angles differ) for 11 of these complexes with simple two-, three-, and four-atom linkages between the azomethine nitrogen donor centers is given in Figure 6. All data refer to copper ions with $d_{x^2-y^2}$ magnetic ground states, and the points denoted \blacktriangle refer to complexes with flat or almost flat dinuclear centers, with no unusual electronic perturbations associated with electron-withdrawing groups in the molecule. These complexes are described in refs 22, 24, 25, 27, and 29 and in the present study (complexes 1, 3). Since there are no unusual structural or electronic perturbations that might be expected to influence exchange in a significant way in these complexes, the phenoxide bridge angle was considered, at least initially, to be the principal factor controlling spin coupling.

The range of averaged angles for these complexes (6.5°) is small and limited mainly by the flexibility of the macrocyclic ligand. In general, as the length of the diamine entity linking the two azomethine nitrogen centers increases, the Cu–O(Ph)–Cu angle increases. The highest average value is 104.7° , which surprisingly compares closely with the maximum value obtained in a series of bis(μ_2 -alkoxide)-bridged dicopper(II) complexes.³ Macrocyclic complexes with high angles ($>102^\circ$) are very strongly coupled with $-2J$ values in the range $815\text{--}905\text{ cm}^{-1}$. Somewhat larger angles ($>103^\circ$) are required for comparable exchange integrals in the alkoxide complexes.^{2,3} A slightly larger angle range ($\approx 7^\circ$) is observed for these systems, and at the lower end of the range ($<98^\circ$), $-2J$ values are quite small and approach 0 cm^{-1} . The overall trend is in qualitative agreement with theoretical calculations for model bis(alkoxide)-bridged systems, using the unrestricted Hartree–Fock method, with corrections for dihedral angles between the coordination planes, distortions at the copper centers, and pyramidal distortions at the oxygen bridge.³ These calculations revealed that the major factor affecting J is the Cu–O–Cu angle. From the data in Figure 6 it is clear that, for the smaller bridge angles

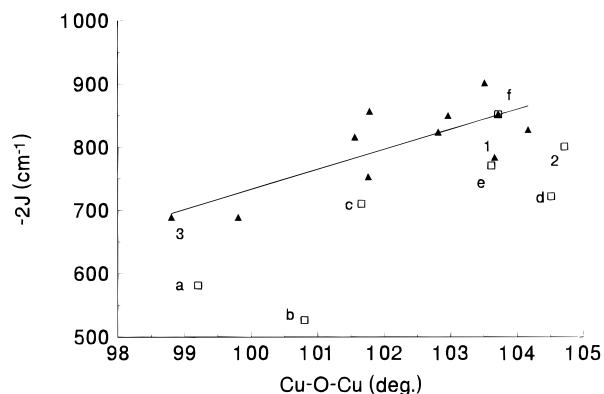


Figure 6. Plot of exchange integral ($-2J$) against Cu–O_{phenoxide}–Cu angle. Points denoted \square refer to complexes with electron-withdrawing groups (identified in the text), and those denoted \blacktriangle are used in the linear regression analysis.

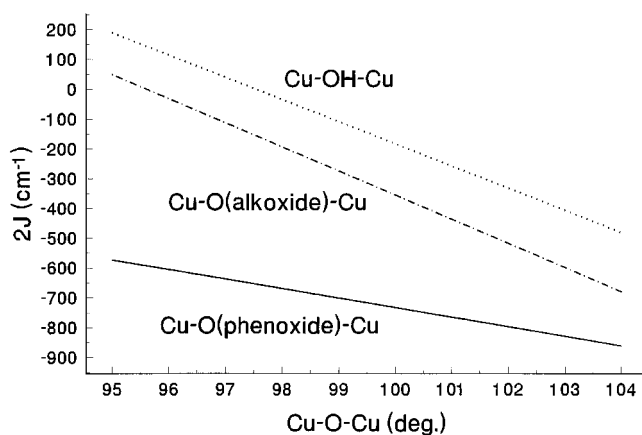


Figure 7. Plot of exchange integral ($-2J$) versus Cu–O–Cu angle for phenoxide-, alkoxide-, and hydroxide-bridged complexes (see text for appropriate references).

($<100^\circ$), $-2J$ values are substantially higher than in the alkoxide or hydroxide cases.

Despite some scatter, the data points (\blacktriangle) in Figure 6 appear to conform to a reasonable straight line. Assuming a linear relationship, the linear least-squares line for these data (Figure 6; \blacktriangle , 11 points) leads to eq 2 (α is the Cu–O–Cu_{av} angle).

$$-2J = 31.95\alpha - 2462\text{ cm}^{-1} \quad (2)$$

What is apparent, and perhaps surprising, is the fact that the least-squares line suggests that antiferromagnetic exchange will dominate in these complexes at angles well below the angle for experimental “accidental orthogonality” established for the dihydroxy-bridged systems¹ and also the dialkoxide-bridged systems.^{2,3} Figure 7 depicts an idealized plot illustrating the three different cases. What is apparent is that the slopes of the hydroxide and alkoxide cases are comparable, but absolute values of $-2J$ are larger for the alkoxides. However, the slope for the phenoxide system is smaller and absolute values of $-2J$ are inherently larger. In contrast to the copper phenoxide situation, a straight-line relationship has been established for comparable dinickel complexes with a similar range of angles, with a projected $-2J = 0\text{ cm}^{-1}$ intercept at $\approx 97^\circ$.⁸ If the larger of the two phenoxide bridge angles is included for those copper cases with asymmetric dinuclear centers, assuming that this might dominate the exchange situation, the slope of the line is less than that in eq 2, which would lead to higher $-2J$ values in the low-angle range. If the straight line given by eq 2 is extrapolated to $-2J = 0\text{ cm}^{-1}$ the Cu–O–Cu angle would be

(24) Tandon, S. S.; Thompson, L. K.; Bridson, J. N. *Inorg. Chem.* **1993**, *32*, 32.

(25) Tandon, S. S.; Thompson, L. K.; Bridson, J. N.; McKee, V.; Downard, A. J. *Inorg. Chem.* **1992**, *31*, 4635.

(26) Mandal, S. K.; Thompson, L. K.; Newlands, M. J.; Gabe, E. J. *Inorg. Chem.* **1990**, *29*, 1324.

(27) Mandal, S. K.; Thompson, L. K.; Nag, K.; Charland, J.-P. *Inorg. Chem.* **1987**, *26*, 1391.

(28) Mandal, S. K.; Thompson, L. K.; Nag, K.; Charland, J.-P.; Gabe, E. J. *Can. J. Chem.* **1987**, *65*, 2815.

(29) Lacroix, P.; Kahn, O.; Theobald, F.; Leroy, J.; Wakselman, C. *Inorg. Chim. Acta* **1988**, *142*, 129.

(30) Hoskins, B. F.; McLeod, N. J.; Schaap, H. A. *Aust. J. Chem.* **1976**, *29*, 515.

(31) Lambert, S. L.; Hendrickson, D. N. *Inorg. Chem.* **1979**, *18*, 2683.

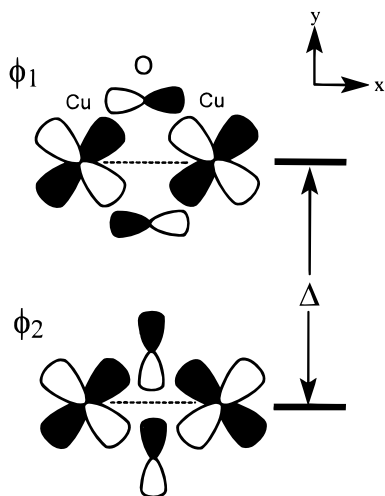


Figure 8. Molecular orbital representation for a Cu_2O_2 framework.

$\approx 77^\circ$, well below the expected value for an oxygen bridge. Since realistic examples of copper complexes with small phenoxide bridge angles ($<97^\circ$) are not available, this magnetic realm cannot be probed experimentally at present. The acetone adduct of **4** has $\text{Cu}-\text{O}-\text{Cu}$ angles $<93^\circ$, but the bending of the molecule along the $\text{O}-\text{O}$ axis and severe pyramidal distortion at the phenoxide oxygens clearly lead to an anomalous magnetic situation (room-temperature magnetic moment of $\approx 1.8 \mu_{\text{B}}$).¹⁸ Also, given the geometrical constraints associated with the macrocycle itself, such angles probably cannot be achieved in an essentially flat system.

To test the role of the phenoxide bridge itself in isolation requires a series of complexes, akin to the hydroxides, with variable bridge angles. To our knowledge, no suitable examples exist involving just a diphenoxide-bridged arrangement with appropriate copper ion ground state. However, the nonmacrocylic complex $[\text{Cu}_2(\text{fsa})_2\text{en}]\cdot\text{CH}_3\text{OH}$ ($\text{H}_4(\text{fsa})_2\text{en} = N,N'$ -bis-(2-hydroxy-3-carboxybenzylidene)-1,2-diaminoethane)³² involves a double phenoxide bridge between two d_{xy} ground state copper(II) centers, and a $\text{Cu}-\text{O}(\text{Ph})-\text{Cu}$ angle of 100.1° . This complex is very strongly antiferromagnetically coupled ($-2J = 650 \text{ cm}^{-1}$) and compares closely with the macrocyclic systems having small bridge angles described in this paper. However $-2J$ is much larger than the values projected from the alkoxide and hydroxide bridge plots (Figure 7). Rationalization of such a situation rests in part with the effect of replacing hydrogen on hydroxide with a more electronegative carbon group, which reduces the electron density on the oxygen bridge. According to Kahn, this mainly affects the oxygen $2p_y$ orbital and makes the $3d_{xy}/2p_y$ molecular orbital less antibonding, resulting in a larger energy gap (Δ) between the two singly occupied molecular orbitals (ϕ_1, ϕ_2) in the triplet state (Figure 8).³² Even though semiquantitative calculations did add some support to this explanation,³² one is reminded of the fact that the difference between the electronegativities of hydrogen and carbon is small (H 2.2, C 2.6; Pauling scale).

An alternative, and apparently untested, explanation involves possible spin exchange between the copper centers via a second bridging route, through the azomethine nitrogens, and the conjugated π framework of the benzene ring. Bis(1,3,5-triketonato)dicopper(II) complexes are known to be very strongly antiferromagnetically coupled, and for a series of 1,5-(R,R')-disubstituted derivatives ($\text{R} = \text{R}' = \text{CH}_3$; $\text{R} = \text{CH}_3$, $\text{R}' = \text{Ph}$; $\text{R} = \text{R}' = \text{CF}_3$), with $\text{Cu}-\text{O}_{\text{ketonate}}-\text{Cu}$ angles in the range

$103-103.5^\circ$, $-2J$ falls in the range $625-740 \text{ cm}^{-1}$.³³⁻³⁵ These levels of antiferromagnetic exchange are somewhat smaller than observed for the phenoxide-bridged macrocyclic complexes under discussion ($-2J_{\text{calc}} = 830 \text{ cm}^{-1}$ for $\text{Cu}-\text{O}-\text{Cu} = 103^\circ$), but the highly delocalized nature of the triketonate groups cannot be ignored in assessing the mechanism for exchange in such complexes. Although this would involve a long exchange distance (a minimal separation of six bonds for both types of complex; $<8 \text{ \AA}$), it is not unreasonable, given the reports of significant antiferromagnetic exchange between square pyramidal copper(II) centers separated by conjugated, aromatic ligands with six bonds (7.6 \AA ; $-2J = 21-26 \text{ cm}^{-1}$),³⁶ eight bonds ($\approx 11.8 \text{ \AA}$; $-J = 36-210 \text{ cm}^{-1}$),³⁷ and nine bonds (11.25 \AA ; $-2J = 140 \text{ cm}^{-1}$).³⁸ Significant antiferromagnetic coupling was also observed between distant ruthenium(III) ions³⁹ (11 bonds), but involving a $d\pi-p\pi$ mechanism. On the assumption that such an antiferromagnetic component might prevail throughout the whole phenoxide angle range in the macrocyclic complexes, it would add a roughly constant component to the total exchange process and thus lead to a situation where, at low phenoxide bridge angles, the actual measured exchange would be more negative (i.e. more antiferromagnetic) than expected. The projected angle for which $-2J = 0 \text{ cm}^{-1}$ would therefore be smaller than for the dihydroxide case or dialkoxide cases, despite the fact that experimental accidental orthogonality for the bridging oxygen might occur close to the expected angle ($\approx 97^\circ$) ($J_{\text{T}} = J_{\text{AF}} + J_{\text{F}}$).

Since the complex $[\text{Cu}_2(\text{fsa})_2\text{en}]\cdot\text{CH}_3\text{OH}$ ³² involves two azomethine linkages in a nonmacrocylic structure, the weaker antiferromagnetic exchange observed (see Figures 6 and 7; eq 2), compared with that of the macrocyclic complexes, which have four such delocalized linkages, would be consistent with a simpler ligand-based exchange route involving just two of these groups. The fact that the dinickel case⁸ appears "normal" by comparison, with a definite change from antiferromagnetic to ferromagnetic behavior at a $\text{Ni}-\text{O}-\text{Ni}$ angle of 97° , is consistent with this argument because the macrocyclic ligands used in this study were all saturated, with no imine linkages to provide the possibility of π -delocalized exchange pathways. One additional factor that can significantly diminish exchange coupling, and which of necessity would be absent in the current systems, is the degree of tetrahedral distortion or dihedral twist angle at the copper centers.⁴⁰ For strong cases of twisting, $-2J$ values can be less than the value predicted for a dihydroxide system with the same angle.¹

The effect of electron-withdrawing substituents bound directly to the copper centers on antiferromagnetic exchange is well documented,^{26,31} with $-2J$ values decreasing with increasing electronegativity, in agreement with Hoffmann's predictions.⁴ However, the effect of electron-withdrawing groups, peripherally bound to e.g. a macrocyclic ligand, is less well documented. The complexes $[\text{Cu}_2(\text{L})](\text{ClO}_4)_2$ ($\text{L} = \text{L6}, \text{L7}$; Figure 1)²³ have $d_{x^2-y^2}$ ground state copper centers in an essentially flat structure with $\text{Cu}-\text{O}-\text{Cu}$ angles of 100.8 and 99.2° , respectively. These

(32) Galy, J.; Jaud, J.; Kahn, O.; Tola, P. *Inorg. Chim. Acta* **1979**, *36*, 229.

(33) Guthrie, J. W.; Lintvedt, R. L.; Glick, M. D. *Inorg. Chem.* **1980**, *19*, 2949.

(34) Lintvedt, R. L.; Glick, M. D.; Tomlonovic, B. K.; Gavel, D. P.; Kuszaj, J. M. *Inorg. Chem.* **1976**, *15*, 1633.

(35) Blake, A. B.; Fraser, L. R. *J. Chem. Soc., Dalton Trans.* **1974**, 2554.

(36) Tinti, F.; Verdager, M.; Kahn, O.; Savariault, J.-M. *Inorg. Chem.* **1987**, *26*, 2380.

(37) Tandon, S. S.; Mandal, S. K.; Thompson, L. K.; Hynes, R. C. *Inorg. Chem.* **1992**, *31*, 2215.

(38) Chaudhuri, P.; Oder, K.; Wiegardt, K.; Gehring, S.; Haase, W.; Nuber, B.; Weiss, J. *J. Am. Chem. Soc.* **1988**, *110*, 3657.

(39) Aquino, M. A. S.; Lee, F. L.; Gabe, E. J.; Greedan, J. E.; Crutchley, R. J. *Inorg. Chem.* **1991**, *30*, 3234.

(40) Chiari, O.; Piovesana, T.; Zanazzi, P. F. *Inorg. Chem.* **1987**, *26*, 952.

complexes have substantially reduced antiferromagnetic exchange ($-2J = 526$ and 581 cm^{-1} , respectively; Figure 6, compounds **b** and **a**), despite the presence of a fully conjugated ligand framework, and this can be attributed to the presence of the four strongly electron-withdrawing fluorine atoms bound to the phenyl linker groups, which generate significant electro-positive character on the copper centers.²³ However, on the basis of the Cu–O–Cu angles, **b** would have been expected to have the larger $-2J$ value. The fact that **a** has the larger value can be attributed to the additional electron-withdrawing influence of the C_3F_7 group in L6, compared with the *tert*-butyl group in L7. Additional support for this subtle difference between $[\text{Cu}_2(\text{L6})](\text{ClO}_4)_2$ and $[\text{Cu}_2(\text{L7})](\text{ClO}_4)_2$ comes from the electrochemical behavior of these complexes, with the reduction potentials occurring at more positive potentials for the L6 (C_3F_7) system.²³ The complex $[\text{Cu}_2(\text{L8})](\text{ClO}_4)_2$ has a comparable structure with a Cu–O–Cu_{av} angle of 101.65° , and an exchange integral ($-2J = 710 \text{ cm}^{-1}$),²⁹ which is again lower than the value predicted from eqn. 2 (Figure 6, compound **c**), as would be expected considering the electron-withdrawing nature of the CF_3 group. The cyano complexes **4** and **5** can be reasonably assumed to have phenoxide bridge angles of $\approx 100^\circ$, by comparison with $[\text{Cu}(\text{L})](\text{ClO}_4)_2$ (L = L6, L7; Figure 1),²³ and so the substantial reduction in antiferromagnetic exchange observed for these complexes, based on their predicted bridge angle, can be associated with the presence of the somewhat remote but strongly electron-withdrawing cyanide groups. Compounds **d–f** (Figure 6) involve ligand L1 (Figure 1), with square pyramidal copper centers and axial halogens (Cl, Br, and I, respectively).^{26,31} For **d**, an early report quoted $-2J = 588 \text{ cm}^{-1}$.³¹ However, we have also reported variable-temperature measurements on this complex ($-2J = 722(20) \text{ cm}^{-1}$)²⁶ and have repeated them in the present study ($-2J = 715(13) \text{ cm}^{-1}$). The iodo complex falls on the line (Figure 6), and so the iodine has little effect, as would be expected, but clearly the presence of bonded chlorine and bromine reduces the antiferromagnetic exchange significantly. **2** is suppressed somewhat, due to the presence of axially bound chlorines in

one molecule, but the effect is diluted by the other molecule in the structure, which has axially bound water molecules. The consistent reduction in antiferromagnetic coupling associated with the presence of directly bound or ligand bound electronegative groups strongly supports the trend established with those complexes for which such groups are absent and also the overall magnetostructural correlation.

Conclusion

A survey of magnetic and structural properties for a number of macrocyclic dinuclear copper(II) complexes with two phenoxide groups bridging the copper(II) centers shows an unexpected linear correlation between bridge angle and exchange in the range $98.8\text{--}104.7^\circ$, very different from that observed for dihydroxide- and dialkoxide-bridged complexes, with strong antiferromagnetic coupling occurring at bridge angles approaching the expected angle of experimental “accidental orthogonality” for these oxygen-bridged complexes. An additional intramolecular antiferromagnetic exchange route via the macrocyclic ligand itself is proposed as a possible way to account for this situation. A series of dicopper complexes of fully saturated forms of L1, L2, and L3 is currently under study as a critical test of the problem regarding the secondary role of the ligand in the exchange process.

Acknowledgment. We thank the Natural Sciences and Engineering Research Council of Canada for financial support for this study, Mr. S. Zhu for magnetic measurements on $[\text{Cu}(\text{L1})\text{Cl}_2]\cdot 2\text{H}_2\text{O}$, and Dr. M. J. Newlands for help with X-ray crystallographic studies. Dr. E. J. Gabe and the National Research Council, Ottawa, are also gratefully acknowledged for providing the use of X-ray facilities.

Supporting Information Available: Tables listing detailed crystallographic data, hydrogen atom positional parameters, anisotropic thermal parameters, and bond lengths and angles for **1–3** and Figure S1, showing the H-bonding framework of **1** (38 pages). Ordering information is given on any current masthead page.

IC9514197